Phosphorescence Quenching of Dyes Adsorbed to Silica Thin-Layer Chromatography Plates

ARTICLE *in* ANALYTICAL CHEMISTRY · JANUARY 2006

Impact Factor: 5.64 · DOI: 10.1021/ac0511703 · Source: PubMed

3 AUTHORS, INCLUDING:

Bao-Hang Han
National Center for Nanoscience and Techno…

100 PUBLICATIONS **3,966** CITATIONS

SEE PROFILE

Anal. Chem. **2005,** *77,* 8075−8085

Phosphorescence Quenching of Dyes Adsorbed to Silica Thin-Layer Chromatography Plates

Bao-Hang Han, Ian Manners, and Mitchell A. Winnik*

Department of Chemistry, University of Toronto, 80 St. George Street, Toronto, ON M5S 3H6, Canada

We describe photoluminescence (PL) quenching experiments by oxygen for a series of transition metal dyes adsorbed to commercial silica thin-layer chromatography plates. These TLC plates have been used by others as rapidly responding PL pressure sensors. The quenching kinetics show interesting differences from the behavior of the same dyes adsorbed to the more well-defined surfaces of SBA-15 mesoporous silica particles adsorbed to a thin layer-by-layer polymer film as reported in *Chem. Mater*. 2005, *17*, 3160. The pore size and the pore size distribution are much larger for the TLC silica than for the mesoporous silica. On the TLC silica, the dye PL decay profiles show smaller deviations from an exponential form. One sees larger differences between the intensity and lifetime Stern−Volmer plots, and most surprisingly, the dyes on the surface of the TLC silica are about three times more sensitive to quenching by oxygen.

In recent years, a need has been identified for air pressure sensors with very fast response. These sensors, for example, would be able to monitor the propagation of shock waves associated with airplanes breaking the sound barrier or due to explosions. One might be interested in the propagation velocity of the initial shock wave or the consequences of the reflection of the shock wave off a variety of surfaces. While there are various possibilities for these kinds of sensors, those based upon a photoluminescence (PL) response have a number of distinct advantages. One can envision passive sensors that are activated by illuminating them at a wavelength where a particular dye in the sensor absorbs light and monitoring the photoluminescence remotely.

On a broader scale, one can imagine an analogue to the types of "pressure-sensitive paints" that are used as two-dimensional air pressure sensors in aviation design. Here one uses a CCD camera to monitor intensity as a function of position for objects in a wind tunnel and converts the intensity profile to a pressure profile. These "paints" consist of dyes incorporated into a polymer film, often as a true solution, but sometimes adsorbed onto colloidal silica particles dispersed in the film. These dye-containing films act as sensors because oxygen diffuses from the surrounding medium into the film. When the dyes become electronically excited upon illumination with light of an appropriate wavelength, quenching of the excited states by oxygen competes with the photoluminescence, leading to a decrease in the intensity of dye emission and an increased rate of excited-state decay. The solubility of oxygen in the polymer increases with the local oxygen partial pressure. Thus, the PL of the dye molecules in the polymer film responds to changes in air pressure at the surface of the film.

Most of the dyes that have been successfully employed as oxygen sensors exhibit phosphorescence at ambient temperature.[1] The most commonly used dyes for these applications have been transition metal porphyrin derivatives such as platinum and palladium porphines[2−9] and ruthenium polypyridyl complexes.[10−17] The most common polymer matrixes have been silicone polymers,[6,10−12,16] chosen for the high oxygen permeability. Our research group has examined the properties of a series of poly(aminothionylphosphazene)s (PATP)[18−25] as a useful matrix for

* To whom correspondence should be addressed. E-mail: mwinnik@chem.utoronto.ca.

(1) (a) Amao, Y. *Microchim. Acta* **2003**, *143* (1), 1−12. (b) Bell, J. H.; Schairer, E. T.; Hand, L. A.; Mehta, R. D. *Annu. Rev. Fluid Mech.* **2001**, *33*, 155−206. (c) Lu, X.; Manners, I.; Winnik, M. A. In *New Trends in Fluorescence Spectroscopy*; Valeur, B., Brochon, J.-C., Eds.; Springer-Verlag: Berlin, 2001; pp 229−255. (d) Lu, X.; Winnik, M. A. In *Organic, Physical, and Materials Photochemistry*; Ramamurthy, V., Schanze, K. S., Eds.; Marcel Dekker Inc.: New York, 2000; pp 311−352. (e) Lu, X.; Winnik, M. A. *Chem. Mater.* **2001**, *13* (10), 3449−3463. (f) Demas, J. N.; DeGraff, B. A. *J. Chem. Educ.* **1997**, *74* (6), 690−695. (g) Gouterman, M. *J. Chem. Educ.* **1997**, *74* (6), 697−702. (h) Guillet, J. E.; Andrews, M. *Macromolecules* **1992**, *25* (10), 2752−2756.
(2) Papkovsky, D. B. *Sens. Actuators, B* **1995**, *29*, 213−218.
(3) Mills, A.; Lepre, A. *Anal. Chem.* **1997**, *69* (22), 4653−4659.
(4) Amao, Y.; Asai, K.; Okura, I.; Shinohara, H.; Nishide, H. *Analyst* **2000**, *125*, 1911−1914.
(5) Douglas, P.; Eaton, K. *Sens. Actuators, B* **2002**, *82*, 200−208.
(6) Lee, S.-K.; Okura, I. *Spectrochim. Acta A* **1998**, *54* (1), 91−100.
(7) Papkovsky, D. B.; Ponomarev, G. V.; Trettnak, W.; O'Leary, P. *Anal. Chem.* **1995**, *67* (22), 4112−4117.
(8) Hartman, P.; Trettnak, W. *Anal. Chem.* **1996**, *68* (15), 2615−2620.
(9) Papkovsky, D. B.; Ovchinnikov, A. N.; Ogurtsov, V. I.; Ponomarev, G. V.; Korpela, T. *Sens. Actuators, B* **1998**, *51*, 137−145.
(10) Kilmant, I.; Wolfbeis, O. S. *Anal. Chem.* **1995**, *67* (18), 3160−3166.
(11) Mills, A. *Sens. Actuators, B* **1998**, *51*, 60−68.
(12) Mills, A. *Sens. Actuators, B* **1998**, *51*, 69−76.
(13) Matsui, K.; Sasaki, K.; Takahashi, N. *Langmuir* **1991** *7* (11), 2866−2868.
(14) Castellano, F. N.; Heimer, T. A.; Tandhasetti, M. T.; Meyer, G. J. *Chem. Mater.* **1994**, *6* (7), 1041−1048.
(15) DellaGuardla, R. A.; Thomas, J. K. *J. Phys. Chem.* **1983**, *87* (6), 990−998.
(16) Xu, W.; McDonough, R. C. III; Langsdorf, B.; Demas, J. N.; DeGraff, B. A. *Anal. Chem.* **1994**, *66* (23), 4133−4141.
(17) Wolfgang, S.; Gafney, H. D. *J. Phys. Chem.* **1983**, *87* (26), 5395−5401.
(18) Yekta, A.; Masoumi, Z.; Winnik, M. A. *Can. J. Chem.* **1995**, *73* (11), 2021−2029.
(19) Pang, Z.; Gu, X.; Yekta, A.; Masoumi, Z.; Coll, J. B.; Winnik, M. A.; Manners, I. *Adv. Mater.* **1996**, *8* (9), 768−771.
(20) Masoumi, Z.; Stoeva, V.; Yekta, A.; Pang, Z.; Manners, I.; Winnik, M. A. *Chem. Phys. Lett.* **1996**, *261*, 551−557.
(21) Masoumi, Z.; Stoeva, V.; Yekta, A.; Winnik, M. A.; Manners, I. In *Polymers and Organic Solids*; Shi, L., Zhu, D., Eds.; Science Press: Beijing, China, 1997; pp 157−168.
(22) Jayarajah, C. N.; Yekta, A.; Manners, I.; Winnik, M. A. *Macromolecules* **2000**, *33* (15), 5693−5701.
(23) Lu, X.; Manners, I.; Winnik, M. A. *Macromolecules* **2001**, *34* (6), 1917−1927.

10.1021/ac0511703 CCC: $30.25
Published on Web 11/15/2005

dye-based oxygen sensor applications.

For PL sensors based on dyes dissolved in liquid films, the response time is limited by the rather slow rate of diffusion of O_2 molecules in the film. Shock tube (pressure jump) experiments by the Sullivan group at Purdue[26] and the Amao group[27] in Japan have shown that solid substrates such as the alumina surface of anodized aluminum and the silica surface of commercial thin-layer chromatography plates provide more rapid response to sudden changes in oxygen partial pressure. These experiments emphasize the need for a better understanding of the factors that affect PL quenching by oxygen for dyes adsorbed to these surfaces.

For most dyes dissolved in simple fluid solvents or dissolved in polymer films at temperatures above the glass transition temperature of the polymer, we understand that the key factors that affect the sensitivity to oxygen quenching include the solubility and diffusion coefficient of oxygen in the host medium and the excited-state lifetime of the dye. For dyes that are adsorbed on solid substrates, we have a much poorer understanding of the factors that affect PL quenching by oxygen. Researchers who have examined oxygen quenching for dyes adsorbed to solid substrates such as silica have found nonexponential PL decay profiles, even in the absence of oxygen. This result suggests that the dyes occupy a distribution of different sites on the surface and that excited dyes at each type of site have their own characteristic decay rate.

Carraway et al.[28] examined oxygen quenching for a series of ruthenium dyes adsorbed to the surface of a porous silica disk prepared from fumed silica. They analyzed their data in terms of two phenomenological models, which we will discuss in more detail below. These models also invoke a distribution of binding sites to accommodate the observation that the quenching response to increasing oxygen partial pressure is more complex than that found for simple liquids.

We recently have become interested in rapidly responding oxygen sensors. In one approach,[29] we prepared SBA-15 mesoporous silica[30] as a promising candidate substrate in which dyes could be bound to the surface of the mesopores. Sensor films were obtained using the layer-by-layer (LbL) self-assembling film method to apply alternating cationic and anionic polyelectrolyte layers to a glass substrate as an adhesion layer, leaving a polycationic surface. A submonolayer of negatively charged mesoporous silica particles was deposited on this film, and dyes were incorporated into the pores by dip coating. These thin-film sensors exhibited intense photoluminescence, a consequence of the high surface area of each silica particle. We then examined the response of the PL intensity and PL decay rate to increasing partial pressures of oxygen.

In this paper, we carry out similar experiments using commercial thin-layer chromatography (TLC) plates as the substrate. These supports are much thicker than the LbL films containing mesoporous silica. The results of the Sullivan group have demonstrated that dyes adsorbed to these TLC plates have intense emission and rapid response to a change in external air or oxygen pressure. We examined a rather broad spectrum of dyes, including platinum and palladium porphines as well as ruthenium bipyridyl and phenanthroline complexes. We were interested in how the excitation and emission spectra compared between the silica gel TLC plates and the mesoporous silica particles. We also examined the breadth of the lifetime distribution in the presence and absence of oxygen, as well as the sensitivity to quenching by oxygen for the various dyes adsorbed to the two substrates.

EXPERIMENTAL SECTION

Instrumentation. Scanning electron microscopy (SEM) images were acquired on a Hitachi S-5200 scanning electron microscope at an acceleration voltage of 10 kV. A small piece of the flexible TLC plate (~6 mm × 8 mm) was cut and attached to the SEM sample holder. Nitrogen sorption ($T = 77$ K) isotherms were obtained with an Autosorb-1 automated gas adsorption analyzer (Quantachrome Instruments). The samples were degassed overnight at 200 °C. Isotherms were evaluated with the Barrett−Joyner−Halenda (BJH) theory[31] to give the porosities, including the Brunauer−Emmett−Teller (BET) surface area,[32] pore volume, pore size, and its distribution.[33]

A homemade device was employed to measure the phosphorescence decay profiles of the dyes adsorbed to the TLC silica film. Here, the third harmonic at 355 nm of a pulsed (10 ns) Nd:YAG laser system (Spectra-Physics GCR-170) operated at 10 Hz was used as the excitation source. The laser beam intensity was severely attenuated through a high-energy variable attenuator (Newport, model 935-10) to prevent sample damage, dye photobleaching, or both. The photoluminescence signal from the dye adsorbed to the TLC silica film was detected by a Hammamatsu 956 photomultiplier tube connected to a Tektronix model 1912 transient digitizer. The decay trace was then digitalized and transferred to a computer for data processing. A SPEX Industries Inc. Fluorolog II model SPEX 1680 spectrometer equipped with a DMA 3000 data system was used to acquire the luminescence spectra and intensities. The air or oxygen pressure was controlled over a range from 0 to 1000 Torr through a combination of a vacuum pump and a compressed gas line. Gas pressure was measured by an MKS Baratron 626A 13TAE absolute pressure transducer with an accuracy of ±0.15% for the range of 10−1000 Torr.

Materials. The TLC plates (20 × 20 cm) were purchased from Whatman Ltd. (Maidstone, Kent, England; made in Germany). The flexible TLC plates contain silica gel (60 Å) with layer

(24) Wang, Z.; McWilliams, A. R.; Evans, C. E. B.; Lu, X.; Chung, S.; Winnik, M. A.; Manners, I. *Adv. Funct. Mater.* **2002**, *12* (6−7), 415−419.

(25) Lu, X.; Han, B.-H.; Winnik, M. A. *J. Phys. Chem. B* **2003**, *107* (48), 13349−13356.

(26) (a) Sakaue, H.; Sullivan, J. P. *AIAA J.* **2001**, *39* (10), 1944−1949. (b) Sakaue, H.; Gregory, J. W.; Sullivan, J. P. *AIAA J.* **2002**, *40* (6), 1094−1098.

(27) Kameda, M.; Tezuka, N.; Hangai, T.; Asai, K.; Nakakita, K.; Amao, Y. *Meas. Sci. Technol.* **2004**, *15*, 489−500.

(28) Carraway, E. R.; Demas, J. N.; DeGraff, B. A. *Langmuir* **1991**, *7* (12), 2991−2998.

(29) Han, B.-H.; Manners, I.; Winnik, M. A. *Chem. Mater.* **2005**, *17* (12), 3160−3171.

(30) (a) Zhao, D.; Feng, J.; Huo, Q.; Melosh, N.; Fredrickson, G. H.; Chmelka, B. F.; Stucky, G. D. *Science* **1998**, *279*, 548−552. (b) Zhao, D.; Huo, Q.; Feng, J.; Chmelka, B. F.; Stucky, G. D. *J. Am. Chem. Soc.* **1998**, *120* (24), 6024−6036. (c) Zhao, D.; Yang, P.; Huo, Q.; Chmelka, B. F.; Stucky, G. D. *Curr. Opin. Solid State Mater. Sci.* **1998**, *3*, 111−121.

(31) Barrett, E. P.; Joyner, L. G.; Halenda, P. P. *J. Am. Chem. Soc.* **1951**, *73* (1), 373−380.

(32) Brunauer, S.; Emmett, P. H.; Teller, E. *J. Am. Chem. Soc.* **1938**, *60* (2), 309−319.

(33) (a) Gregg, S. J.; Sing, K. S. W. *Adsorption, Surface Area and Porosity*, 2nd ed.; Academic Press: London, 1982. (b) Sing, K. S. W.; Everett, D. H.; Haul, R. A. W.; Moscou, L.; Pierotti, R. A.; Rouquérol, J.; Siemieniewska, T. *Pure Appl. Chem.* **1985**, *57* (4), 603−619.

thickness of 250 μm supported by aluminum flexible backing and contained no fluorescent indicator. These plates could readily be cut into smaller pieces (~2 × 2.5 cm) for the preparation of oxygen sensor films.

The dyes 2,3,7,8,12,13,17,18-octaethyl-21*H*,23*H*-porphineplatinum(II) (or platinum(II) octaethylporphine, PtOEP), platinum(II) meso-tetraphenylporphine (PtTPP), and platinum meso-tetrakis(pentafluorophenyl)porphine (PtTFPP) were purchased from Porphyrin Products, Frontier Scientific Inc. (Logan, UT). 2,3,7,8,12,13,17,18-Octaethyl-21*H*,23*H*-porphinepalladium(II) (or palladium(II) octaethylporphine, PdOEP), tris(1,10-phenanthroline)ruthenium(II) dichloride hydrate ($[Ru(phen)_3]Cl_2$), and tris(2,2′-bipyridyl)ruthenium(II) dichloride hexahydrate ($[Ru(bpy)_3]Cl_2$) were purchased from Aldrich. All the above dyes were used without further purification. Tris(4,7-diphenyl-1,10-phenanthroline)-ruthenium(II) dichloride ($[Ru(dpp)_3]Cl_2$), and $[Ru(phen)_2phenCH_3]Cl_2$ (phen=1,10-phenanthroline, $phenCH_3$ = 4-methyl- 1,10-phenanthroline) were synthesized in Prof. I. Manners' group according to a literature procedure.[34]

1,1,1-Trichloroethane (TCE, 99+%) and methanol (99%) were obtained from Aldrich. Deionized water (>10 MΩ cm) was obtained through the treatment of distilled water by a MilliQ water system. Oxygen (Research Grade 4.7, 99.997%) and compressed dry air (impurity H_2O 10 ppm) were obtained from BOC gas.

Dye Loading on TLC Silica Films. The dyes were incorporated into the TLC silica films by dipping them for ~2 min into clear solutions of the dyes at a concentration of $\sim 10^{-4}$ M in various solvents. The platinum dyes were dissolved in TCE, while $[Ru(dpp)_3]Cl_2$ was dissolved in methanol, and the other three ruthenium dyes were dissolved in deionized water. The films were then allowed to dry in the dark at room temperature overnight. The films obtained were subjected to vacuum (~0.2 Torr) at ambient temperature for 12 h and then used directly in the photoluminescence measurements.

Phosphorescence Intensity and Decay Measurements. Luminescence emission intensity measurements were carried out using a time-scan approach for signal averaging as reported elsewhere.[29] When acquiring the luminescence decay profiles of excited-state dyes, a filter BP300-400 was placed in the excitation beam path before the film sample and the emission was passed through another appropriate filter CO470 placed before the detector in order to eliminate scattered excitation light. A homemade vacuum/pressure sample chamber was used, in which the pressure was controlled by an air or oxygen cylinder and a vacuum line.

Data Analysis. In ideal fluid solutions, luminescence intensities and decay times for quenching by oxygen follow the simple Stern−Volmer equation.[35]

$$\frac{I^o}{I} = \frac{\tau^o}{\tau} = 1 + k_q \tau^o [Q] \qquad (1)$$

where I^o, I, and τ^o, τ are the luminescence intensities and the luminescence decay lifetimes in the absence and in the presence of quencher. [Q] denotes the concentration of the quencher, and k_q is the rate constant of the bimolecular quenching reaction. When the quencher is a gas such as oxygen, and for fluid systems where Henry's law applies, the luminescence intensity will be proportional to the partial pressure of oxygen, p_{O_2}. A similar proportionality is predicted for quenching preceded by gas adsorption to a solid surface, if adsorption follows a Langmuir isotherm, and the experiments are carried out far from saturation. Under these circumstances

$$\frac{I^o}{I} = 1 + K_{SV} p_{O_2} \qquad (2)$$

where the Stern−Volmer constant K_{sv} contains all of the proportionality constants relating the oxygen pressure to the luminescence intensity.

Dyes in homogeneous solutions normally exhibit simple exponential luminescence decays. For dyes adsorbed to silica surfaces, PL decays are often nonexponential. Under these circumstances, one can fit the decay profiles to a sum of exponential terms

$$I(t) = \sum_i A_i \exp\left(-\frac{t}{\tau_i}\right) \qquad (3)$$

where $I(t)$ is the luminescence intensity at time t and A_i is the normalized preexponential factor for the ith species with a lifetime τ_i. "Intensity-averaged" mean lifetimes $\langle\tau\rangle$ were calculated from the expression

$$\langle\tau\rangle = \sum_i A_i \tau_i \qquad (4)$$

RESULTS AND DISCUSSION

Preparation and Characterization of the Silica TLC Film Containing Dye. We begin with a brief characterization of the silica on the TLC plate. SEM images at two different magnifications of the TLC surface are shown in Figure 1. The silica appears to be in the form of leaflike or blocklike objects with dimensions on the order of 10−20 μm. The surface is rough, and there is an internal structure that cannot be seen in these images. To characterize the porosity of the silica gel, the nitrogen adsorption−desorption isotherm was measured, with the results shown in Figure 2. Nitrogen condensation occurred in the relative pressure range of 0.4−0.85. This wide range of pressures indicates that the TLC silica gel is characterized by a very wide pore size distribution. The inset in Figure 2 shows the BJH pore size distribution[31] calculated from the adsorption and desorption branches of the isotherm. This plot confirms the wide pore size distribution. The BET surface area[32] of the silica is 340 m^2/g, and the pore volume is 0.68 cm^3/g at the relative pressure of 0.95. In contrast, the mesoporous SBA-15 silica[36] that we examined previously[29] was characterized by well-defined cylindrical particles with a BET surface area of 960 m^2/g and a pore volume of 1.24 cm^3/g at the relative pressure of 0.95.

(34) Lin, C.-T.; Böttcher, W.; Chou, M.; Creutz, C.; Sutin, N. *J. Am. Chem. Soc.* **1976**, *98* (21), 6536−6544.

(35) Lakowicz, J. R. *Principles of Fluorescence Spectroscopy*, 2nd ed.; Kluwer Academic/Plenum Publishers: New York, 1999.

(36) Sayari, A.; Han, B.-H.; Yang, Y. *J. Am. Chem. Soc.* **2004**, *126* (44), 14348−14349.

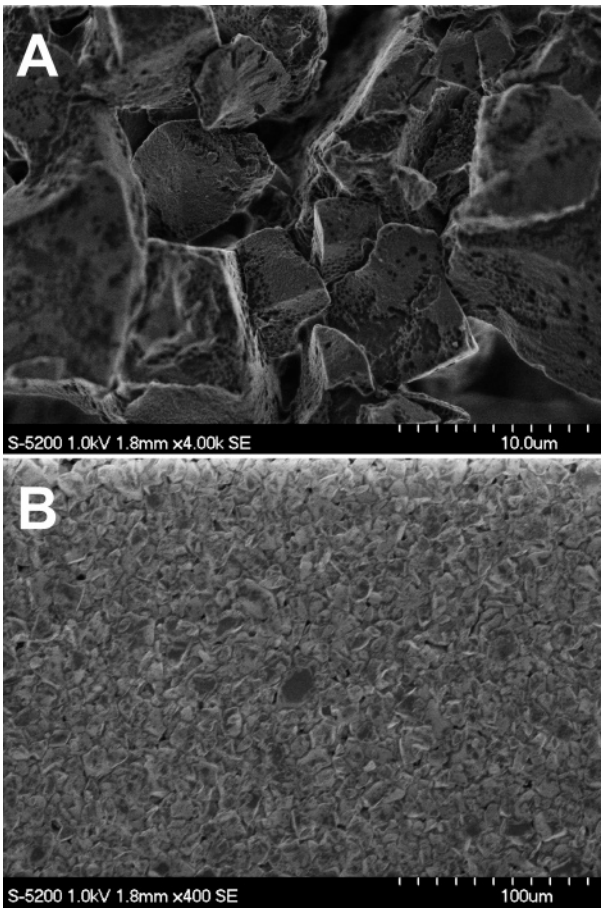

Figure 1. SEM images at two levels of magnification of the surface of the silica TLC plates used as sensors.

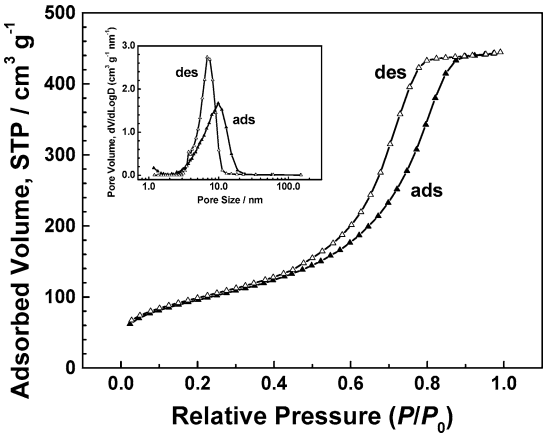

Figure 2. Nitrogen adsorption−desorption isotherms for the silica gel from the silica TLC plates. Inset: BJH pore size distribution obtained from the adsorption and desorption branches, respectively. (adsorption (ads), solid triangles; desorption (des), open triangles).

The dyes were incorporated into the TLC silica films by dipping them for ~2 min into clear solutions of the dyes at a concentration of $\sim 10^{-4}$ M in various solvents. The molecular structures of these dyes are shown in Chart 1. The porphyrin dyes (PtOEP, PdOEP, PtTFPP, PtTPP) were dissolved in TCE, while $[Ru(dpp)_3]Cl_2$ was dissolved in methanol, and the other three ruthenium dyes ($[Ru(phen)_2phenCH_3]Cl_2$, $[Ru(phen)_3]Cl_2$, $[Ru(bpy)_3]Cl_2$) were dissolved in deionized water. We note that it is not easy to determine the amount or concentration of dye adsorbed to the sample. Solutions that were too dilute or dipping times that were too short gave films with weak dye luminescence intensity. We chose conditions for which the emission intensity was strong and for which the PL spectrum was unaffected by small variations in either dye concentration in the solution or dipping time. The films were dried in the dark exposed to air. Before each PL measurement, the film sample was placed in the sample holder, which was then evacuated to ~0.2 Torr, with continued pumping for a minimum

Chart 1

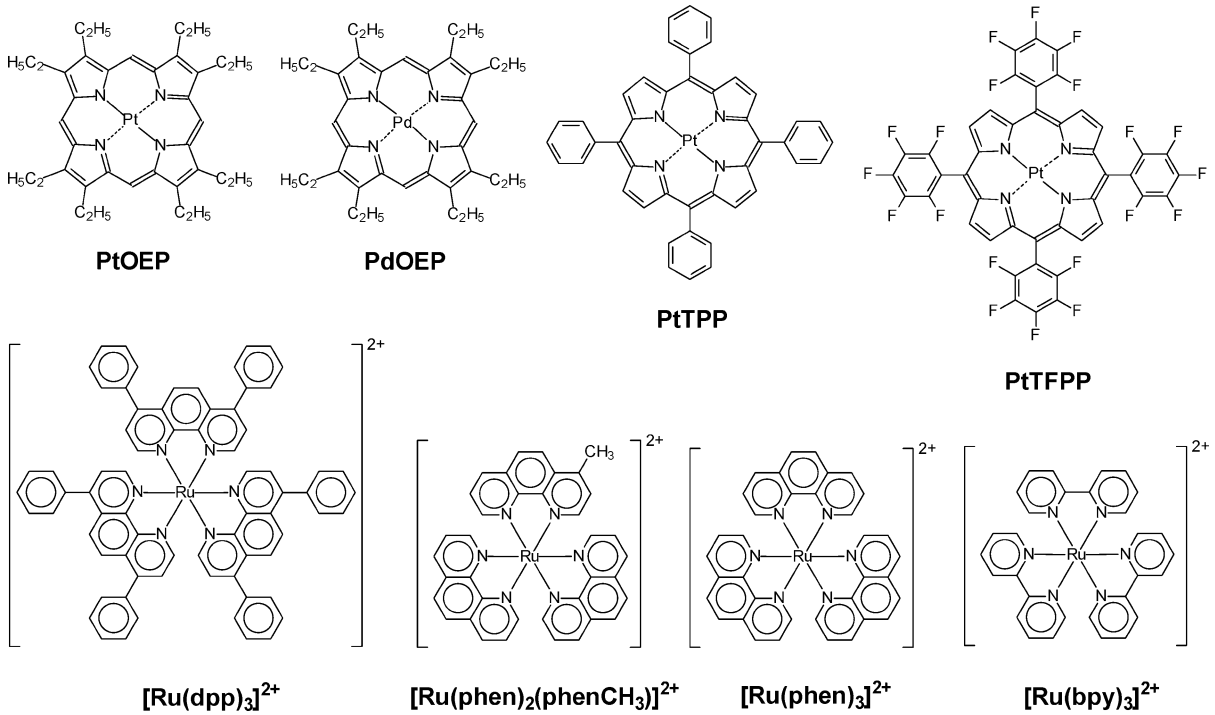

Table 1. Excitation, Emission Peak Positions, and Unquenched Average Lifetimes of Various Dyes in the TLC Silica Film and the Mesoporous Silica Particles

	TLC silica film						mesoporous silica particles [a]					
	$\lambda_{ex.max}$ [b]	$\lambda_{em.max}$ [b]	$\langle\tau\rangle^{\circ}$ [c]	$\tau_m{}^{\circ}$ [c]	γ	αR_{eff} [b]	$\lambda_{ex.max}$ [b]	$\lambda_{em.max}$ [b]	$\langle\tau\rangle^{\circ}$ [c]	$\tau_m{}^{\circ}$ [c]	γ	αR_{eff} [b]
PdOEP	393	665	1000	935	0.55	0.80	393	664	1000	687	0.94	0.38
PtOEP	383	647	97.8[d]	95.0	0.39	1.0	381	646	84.4	81.3	0.66	1.0
PtTFPP	391	649	76.9[d]	76.7	0.09	0.47	391	649	71.2	70.3	0.28	0.42
PtTPP	398	662	81.4[d]	81.1	0.12	0.80	400	661	77.6	74.3	0.72	0.45
$[Ru(dpp)_3]Cl_2$	465	607	8.14	7.90	0.37	0.95	465	603	7.56	7.11	0.48	0.90
$[Ru(phen_2phenCH_3)]Cl_2$	452	591	5.84	5.13	0.25	2.5	452	591	3.75	3.33	0.75	0.88
$[Ru(phen)_3]Cl_2$	451	590	4.54	4.25	0.49	2.8	451	586	2.99	2.67	0.73	1.25
$[Ru(bpy)_3]Cl_2$	452	600	1.74[d]	1.74	0.11	2.2	452	600	1.40[d]	1.40	0.14	1.12

[a] Reference 29. [b] Unit, nm. [c] Unit, μs. [d] Unquenched lifetime (τ°) from single-exponential decay.

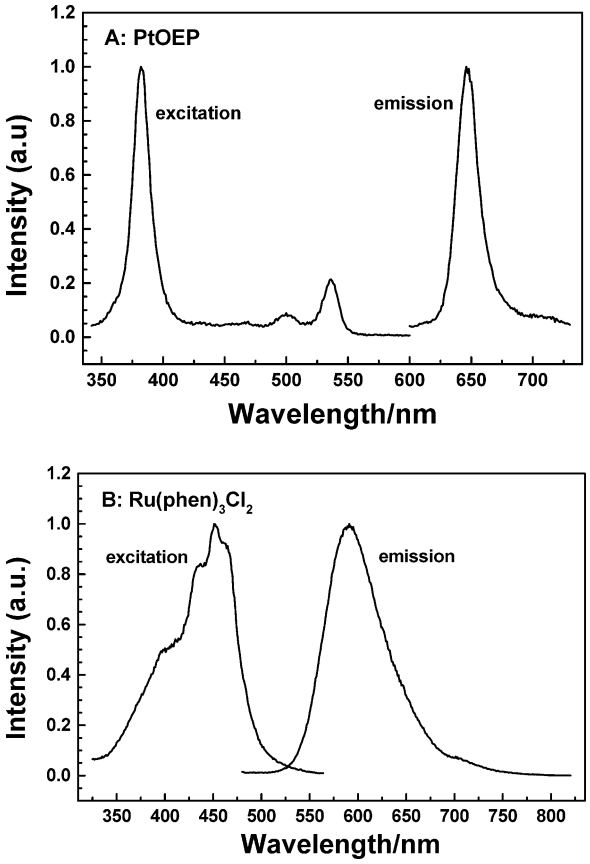

Figure 3. Emission and excitation spectra of PtOEP (A) and $[Ru(phen)_3]Cl_2$ (B) adsorbed on the silica TLC plates.

of 12 h overnight. This was the procedure used to remove oxygen and loosely bound solvent or water from the silica surface.

Properties of the Dyes Adsorbed to the Silica TLC Plates. In our previous paper on dyes adsorbed to SBA-15 silica, we noted that the excitation and emission spectra of these dyes were similar to the corresponding spectra of the same dyes dissolved in films of poly(*n*-butyl thionylphosphazene) (C_4PATP). C_4PATP can be thought of as a polar aprotic solvent (like *N*-methylpyrrolidone) effective at dissolving metalloporphine dyes and ionic ruthenium dyes. The emission and excitation spectra of PtOEP and $[Ru(dpp)_3]Cl_2$ adsorbed on a TLC silica film are shown in Figure 3. The main excitation and emission peak wavelengths for the eight transition metal complex dyes adsorbed on the TLC silica ($\lambda_{ex,max}$, $\lambda_{em,max}$) are listed in Table 1. Also listed in the table for comparison are the corresponding peak positions of the dyes adsorbed on the mesoporous silica particles. Here we note that the excitation and emission spectra of these dyes adsorbed to the TLC silica are essentially the same as those adsorbed to the mesoporous silica. From this information, we conclude that the dyes adsorb to the silica in a molecularly discrete state rather than as dye aggregates.

A curious feature of the dyes adsorbed to TLC silica is that many of the PL decay profiles show only small deviations from a simple exponential profile, particularly in the absence of oxygen. For example, the phosphorescence decay profiles obtained for the three platinum dyes (PtOEP, PtTFPP, PtTPP) and one ruthenium(II) dye ($[Ru(bpy)_3]Cl_2$) adsorbed on the TLC silica film are single-exponential in the absence of oxygen. While the luminescence decay profiles for the other dyes (PdOEP, $[Ru(dpp)_3]Cl_2$, $[Ru(phen)_2phenCH_3]Cl_2$, $[Ru(phen)_3]Cl_2$) are nonexponential in the absence of oxygen, they are easily fitted with a sum of two exponential terms. This result stands in contrast to the result reported by Carraway et al.[28] that the ruthenium dyes on fumed silica exhibited such strong deviations from exponential behavior that a sum of three or four exponential terms (cf. eq 3) was needed to fit the decays. The values of the "unquenched" lifetimes or mean lifetimes obtained for TLC silica are listed in Table 1 and compared to those obtained for the mesoporous silica.

PL Quenching Experiments. When the oxygen partial pressure in the sample chamber was increased, the emission intensity of the dyes decreased. The global behavior of all of the dyes was similar, but the sensitivity to a change in oxygen partial pressure varied from dye to dye. As a rule, the longer the unquenched lifetime, the more sensitive the dye was to quenching by oxygen. The emission peak at 646 nm for PtOEP decreases in intensity but does not shift or change in shape over the entire pressure range investigated. In contrast, the emission peak for $[Ru(phen)_3]Cl_2$ shifts from 590 nm in the absence of oxygen to 583 nm in the presence of 750 Torr oxygen. This hypsochromic shift indicates that the $[Ru(phen)_3]Cl_2$ dyes that are the most difficult to quench are in an environment that leads to a blue-shifted emission spectrum.

To improve the precision for PL intensity measurements for quantitative analysis of the oxygen quenching data, intensities were measured at λ_{max} using the time-base scan mode of the instrument. Intensities obtained over 100−300 s were averaged. The relative error is very small, typically <2% of the mean intensity. Stern−Volmer plots were constructed (eq 2) by plotting

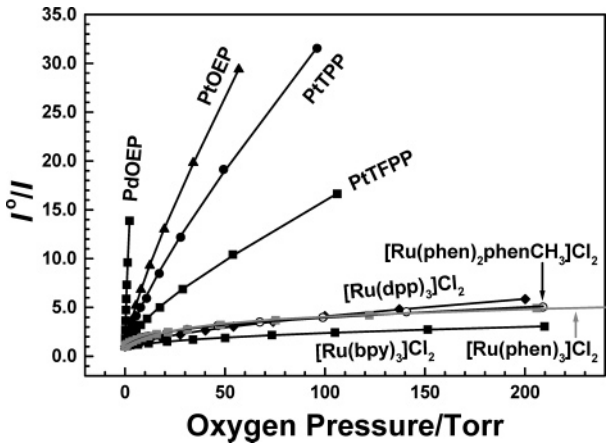

Figure 4. Intensity Stern–Volmer plots for four porphyrin dyes and four ruthenium dyes adsorbed on the silica TLC plates.

I^o/I versus p_{O_2}. These plots are shown in Figure 4. All of the plots show curvature in the low-pressure range, but become more linear at higher pressures. This type of curved Stern–Volmer plot has been observed previously and has been attributed to site heterogeneity for the dyes.[37] For simple systems in solution (eq 1), K_{sv} is proportional to the unquenched lifetime τ^o. For oxygen quenching of pyrene and 9,10-diphenylanthracene adsorbed to a commercial Cab-O-Sil silica (HS-5),[38] the Thomas group found that the SV plots could be made to superimpose using τ^o as a scaling parameter. We tested this idea (see Figure S1A in Supporting Information) by plotting $(1/\tau^o)(I^o/I - 1)$ versus p_{O_2}. We found that while normalization by τ^o reduced the differences among the various SV plots, other factors must also play a role in determining the quenching kinetics.

Comparison with Mesoporous Silica. In this section, we compare the quenching efficiency of oxygen for the dyes adsorbed to TLC silica with the quenching efficiency determined previously for the same set of dyes in which the substrate was SBA-15 mesoporous silica, [29] and the samples were prepared in a similar way. In Table 1, we summarize many of the properties of the dyes adsorbed to the mesoporous silica and compare these properties to those of the dyes absorbed to the TLC silica that we examine here. The first feature that one notices is that the absorption and emission wavelengths of the dyes are very similar. The unquenched lifetimes are also similar, although in most instances, the mean lifetimes of the dyes on the mesoporous silica are somewhat shorter than on the TLC silica. The unquenched decays on the TLC silica show smaller deviations from an exponential profile, and four of the dyes on the TLC plate have unquenched decays that fit well to a simple exponential form. Taken together, these results indicate that there is a somewhat narrower distribution of binding sites for dyes on TLC silica than for the mesoporous silica sample we examined previously.

In Figure S1B (Supporting Information), as a comparison, we reproduce from ref 29 the plot of the lifetime-normalized values of intensity changes $[(1/\tau^o)(I^o/I - 1)]$ induced by exposure of the mesoporous silica film samples to various partial pressures of oxygen. Overall, the shapes of the plots resemble those for the dyes on the TLC silica (Figure S1A). The lifetime itself as a scaling parameter does not reduce the quenching data to a single curve. While there are some small differences in curve shape for individual dyes between Figures S1A and B, the most striking difference is in the magnitude of quenching for the two substrates. For a given oxygen pressure, the magnitude of the *y*-axis for the TLC plate is two to three times as large as that for the mesoporous silica. The data in Table 1 indicate that this difference is not due to differences in the unquenched lifetime $\langle\tau^o\rangle$. Rather, dyes on the TLC substrate are more sensitive to quenching by oxygen. We will return to this point later in the paper.

PL Decay Experiments. PL decay profiles as a function of p_{O_2} were measured for five of the eight dyes. Because of instrument limitations, these experiments were not carried out for the ruthenium dyes ($[Ru(phen)_2phenCH_3]Cl_2$, $[Ru(phen)_3]Cl_2$, $[Ru(bpy)_3]Cl_2$) with the shortest lifetimes. PL decay profiles of PtOEP, PtTPP and $[Ru(dpp)_3]Cl_2$ adsorbed on TLC silica at various oxygen partial pressures are presented in Supporting Information (Figure S2). The behavior seen is typical for all dyes examined. As mentioned above, the PL decays of PtOEP, PtTFPP, and PtTPP are exponential in the absence of oxygen. Deviations from exponential behavior are difficult to detect at low oxygen pressures, but at higher pressures, curvature can be seen in the semilogarithmic plots, and two exponential terms are necessary to fit the decays. For PdOEP and $[Ru(dpp)_3]Cl_2$, none of the decay profiles were exponential. The deviations were small at low oxygen pressure but became more pronounced as the oxygen pressure was increased.

According to eqs 1 and 2, for simple systems, lifetime SV plots should be coincident with intensity SV plots. To test this idea, we plot $\tau^o/\langle\tau\rangle$ for dyes with exponential unquenched decays and for $\langle\tau^o\rangle/\langle\tau\rangle$ dyes with nonexponential unquenched decays. Three examples are shown in Figure 5. For PtOEP, the $\langle\tau^o\rangle/\langle\tau\rangle$ and I^o/I values coincide over almost the entire pressure range where lifetime data were obtained. There is a suggestion of a small downward curvature in the lifetime plot at the highest oxygen pressure (p_{O_2} = 20 Torr). For PtTPP, the two plots superimpose only in the low range of oxygen pressures, less than 10 Torr. For $[Ru(dpp)_3]Cl_2$, the lifetime data lie below the intensity data over the entire pressure range of the experiment. The data for PtTFPP (not shown) resemble more the data for PtOEP. The two plots superimpose for quenching to ~80% of the luminescence but diverge at higher pressures. For each of these dyes, the intensity plots show less curvature at high pressure than the lifetime plots. Behavior similar to that seen in Figure 5B was reported previously by Carraway et al.[28] for ruthenium dyes adsorbed to a pressed disk formed from fumed silica.

It is difficult to provide an unambiguous explanation for this type of behavior. The most common explanation for an experiment in which a quencher has a larger effect on the PL intensity than on the lifetime is that static quenching plays a role. The term "static quenching" refers to the situation in which some quenchers are adjacent to dye molecules prior to excitation. Upon excitation, these dyes are quenched so quickly that they do not contribute to the signal used to measure the lifetime. This type of explanation

(37) (a) Demas, J. N.; DeGraff, B. A.; Coleman, P. A. *Anal. Chem.* **1999**, *71*, 793A–800A. (b) Demas, J. N.; DeGraff, B. A.; Xu, W. *Anal. Chem.* **1995**, *67* (8), 1377–1380. (c) Carraway, E. R.; Demas, J. N.; DeGraff, B. A.; Bacon, J. R. *Anal. Chem.* **1991**, *63* (4), 337–342. (d) Carraway, E. R.; Demas, J. N.; DeGraff, B. A. *Anal. Chem.* **1991**, *63* (4), 332–336.

(38) Krasnansky, R.; Koike, K.; Thomas, J. K. *J. Phys. Chem.* **1990**, *94* (11), 4521–4528.

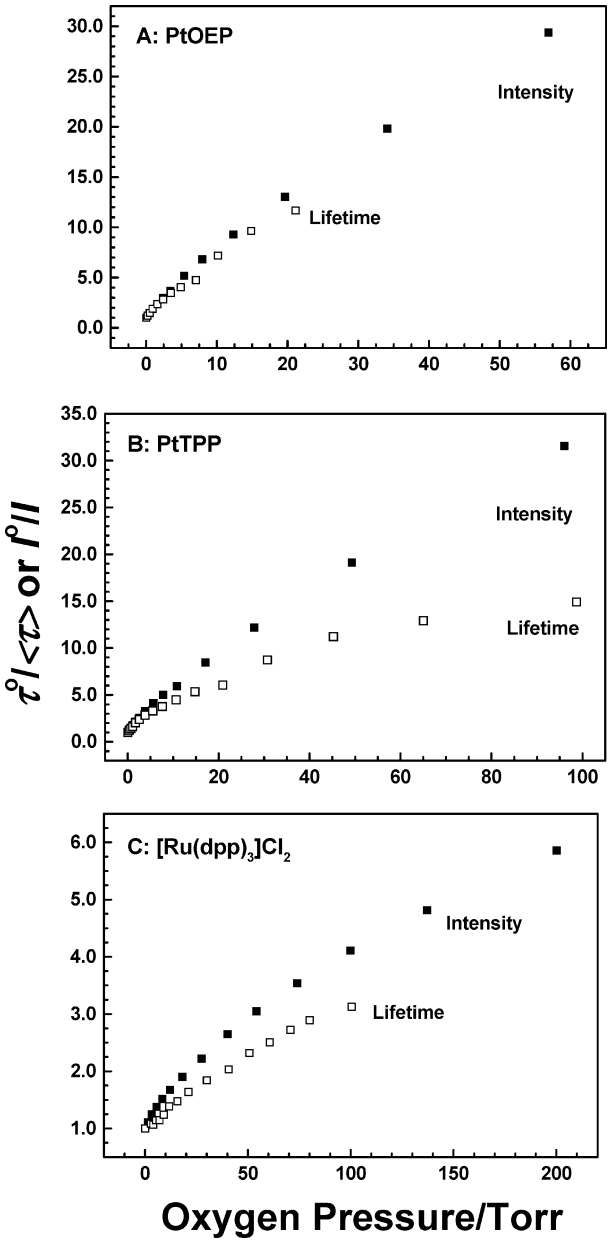

Figure 5. Comparison of intensity and lifetime Stern−Volmer plots for three dyes adsorbed on the silica TLC plates.

might explain enhanced intensity quenching at high partial oxygen pressures but will not explain the data in Figure 5B or C.

Models for Phosphorescence Quenching. Curved Stern−Volmer plots are not consistent with the simple models that underlie eqs 1 and 2. Phenomenological models have been proposed to account for the curvature in the intensity SV plots, but these have not been extended to also account for differences between the intensity and lifetime data. Krasnansky et al.[38] have employed a more quantitative approach to explaining fluorescence quenching by oxygen for pyrene and diphenylanthracene adsorbed to silica. We will look briefly at each of these models in turn.

These models assume that diffusion of oxygen bound to the surface of the silica is responsible for the quenching process. The surface concentration of quencher $[Q]_{ads}$ depends on the external oxygen pressure through the adsorption isotherm. Krasnansky et al.[38] carried out oxygen isotherm measurements at a series of low temperatures where good data could be obtained and showed that oxygen adsorption followed a simple Langmuir isotherm. In the Langmuir isotherm, the fractional surface coverage θ is related to p_{O_2} through the expression

$$\theta = \frac{[Q]_{ads}}{[Q]_{max}} = \frac{bp_{O_2}}{1 + bp_{O_2}} \tag{5}$$

where $[Q]_{max}$ is the maximum surface concentration (presumably a monolayer) and b is related to the adsorbate adsorption energy. The Langmuir model assumes that all binding sites have the same binding energy.

The Freundlich isotherm adsorption model is an extension of the Langmuir model and supposes that there is a distribution of site energies with preferential binding to the most energetic sites. The model leads to an expression of the form

$$\theta = a{p_{O_2}}^{1/n} \tag{6}$$

for gas−solid adsorption. Here a represents a series of constants and n is an empirical parameter. Carraway et al.[28] measured the oxygen-binding isotherms to their silica disks, but for the low fractional surface coverage accessible in their experiments, they could not distinguish a simple Langmuir isotherm (eq 5) from the more general Freundlich isotherm.

Two-Site Model. Carraway et al.[28] have shown that the curvature in an SV plot can be described by a simple two-site model. In this model, one assumes that there are two distinct sets of sites for the dye in the system. The more sensitive sites are characterized by an SV constant K_{sv1} and f_1 is the fraction of such sites. The other dyes $(1-f_1)$ occupy a second set of sites characterized by K_{sv2}. The appropriate expression used to fit the data is

$$\frac{I^o}{I} = \frac{1}{\dfrac{f_1}{1 + K_{SV1}p_{O_2}} + \dfrac{1 - f_1}{1 + K_{SV_2}p_{O_2}}} \tag{7}$$

Implicit in this model is that the surface concentration of O_2 is proportional to p_{O_2} and that the two SV constants adequately describe the curvature of the SV plots. This model is phenomenological because one does not insist that there are only two well-defined sites for the dye. Rather, this model is used as a more general description of a distribution of sites that have different sensitivities to quenching by oxygen. As defined, f_1 and $(1-f_1)$ refer to the distribution of dyes, and K_{sv1} and K_{sv2} refer to their susceptibility to quenching, as reflected perhaps in their unquenched lifetimes. The lines passing through the data points in Figure 4 represent fits to this model. This model fits the data rather well. The fitting parameters obtained are listed in Table 2. The values of the fraction f_1 for the four porphyrin dyes are reasonably close to each other and range from 0.89 to 0.96. For the ruthenium(II) dyes, the values of f_1 range from 0.63 and 0.78. The K_{sv1} values tend to track the unquenched lifetimes, and the K_{sv2} values are much smaller than K_{sv1}. But within the ruthenium dyes, the quenching sensitivity of $[Ru(dpp)_3]Cl_2$ is comparable to

Table 2. Comparison of Stern–Volmer Constants for Various Dyes in the TLC Silica Films Obtained from the Fitting Employing Different Model, i.e., Two-Site Model and Freundlich Adsorption Model

	Demas–DeGraff two-site model				Freundlich adsorption model		
	f_1	K_{sv1}/Torr^{-1}	K_{sv2}/Torr^{-1}	χ^2	K'_{sv}	$1/n$	χ^2
PdOEP	0.95	9.94	0.26	0.03021	6.73	0.80	0.05965
PtOEP	0.85	0.47	0.0050	0.00183	0.61	0.56	0.03127
PtTFPP	0.89	0.41	0.016	0.0037	0.46	0.76	0.00241
PtTPP	0.96	0.61	0.018	0.03716	0.75	0.81	0.01658
$[Ru(dpp)_3]Cl_2$	0.79	0.080	0.0037	0.00112	0.13	0.69	0.00229
$[Ru(phen_2phenCH_3)]Cl_2$	0.73	0.20	0.0026	0.00431	0.31	0.49	0.00885
$[Ru(phen)_3]Cl_2$	0.72	0.21	0.0025	0.00416	0.34	0.47	0.00918
$[Ru(bpy)_3]Cl_2$	0.63	0.049	0.0017	0.00051	0.081	0.61	0.00146

or slightly smaller than those of $[Ru(phen)_3]Cl_2$ and $[Ru(phen)_2phenCH_3]Cl_2$.

Freundlich Isotherm Model. An alternative approach to describing the curvature in the SV plots can be developed in terms of a model involving a single SV constant in combination with an oxygen-binding isotherm that has a nonlinear dependence on p_{O_2}. These ideas, in conjunction with a Freundlich isotherm for oxygen lead to a SV expression of the form

$$\frac{I^o}{I} = 1 + K_{SV}[O_2]_{max}\, a p_{O_2}{}^{1/n} = 1 + K'_{SV} p_{O_2}{}^{1/n} \qquad (8)$$

Here K'_{SV} is a fitting parameter that represents the product of K_{SV} and the constants $a[O_2]_{max}$. Carraway et al.[28] showed that this model was very effective at fitting intensity SV data for the various ruthenium(II) dyes adsorbed on the porous disks they prepared from fumed silica. In our experiments on mesoporous silica, we also found that this model was as effective as the two-site model in fitting I^o/I data for all of the dyes we examined. We obtained similar results here. The quality of the fitting for data fitted to eq 8 was comparable to that obtained for the two-site model. We list the fitting parameters in Table 2. The $1/n$ values obtained fall in the range 0.47–0.80, implying, if this model were correct, a strongly nonlinear adsorption isotherm for oxygen.

Gaussian Distribution Model. The Gaussian distribution model provides a way for analyzing nonexponential PL decay curves. The fundamental assumption is that the dyes have a distribution of environments on the surface and that these sites are characterized by a distribution of decay rates. This is the situation encountered by Krasnansky et al.[38] in their study of fluorescence quenching by O_2 of two dyes adsorbed to the surface of their silica particles. They invoked the assumption of a Gaussian distribution of decay rates,[39] characterized by a mean decay rate $k_m = 1/\tau_m$ and a distribution parameter γ. In this model, the dispersion in the first-order rate constants for $-\infty \le x \le \infty$ is given by the expression

$$\ln(k) = \ln(k_m) + \gamma x \qquad (9)$$

From their isotherm data, they calculated the surface concentration of adsorbed oxygen ($[O_2]_{ads}$) and showed that their experiments at all temperatures were consistent with a quenching rate expression of the form

$$\frac{1}{\tau_m} = \frac{1}{\tau_m^\circ} + k_q'[O_2]_{ads} \qquad (10)$$

where $1/\tau_m^\circ$ is the Gaussian mean decay rate for the dye in the absence of oxygen and k'_q is the second-order quenching rate constant. Plots of $1/\tau_m$ against oxygen surface concentration were linear and increased with temperature. This result shows that the steeper SV slopes at low temperature were due to an enhanced oxygen surface concentration and not a fundamental change in quenching mechanism. The calculated Arrhenius activation energy for k'_q was close in magnitude to the binding energy of oxygen on the surface of the silica.

We fitted each of our measured decay profiles to the Gaussian distribution model. Not having measured oxygen-binding isotherms, we confine ourselves to comments about the nature of the fit of our data to this model. In Table 1, we list values of τ_m° for each dye and note that these values are close in magnitude to τ^o or $\langle\tau^o\rangle$ calculated from eq 4.[40] Because most of the unquenched decays are exponential or nearly exponential, values of the fitting parameter γ are small. What is really surprising is the strong increase in γ for the Pd and Pt porphine dyes with small increases in p_{O_2}. These results are shown in Figure 6B, where one can see that γ increases from values close to zero to values close to 1 over a few Torr increase in pressure. To emphasize the response of the fitting parameter γ to small changes in p_{O_2}, we expand the x-axis scale for these data in Figure 6C. Here one can see that the range of pressures over which γ increases is somehow connected to the lifetime of the dye, with the most rapid increase for the Pd dye.

If eq 10 provides a full and proper description of the system and oxygen adsorption follows a Langmuir isotherm, one would expect that plots of $1/\tau_m$ versus p_{O_2} would be linear with a slope proportional to k'_q. As shown in Figure 6A, this plot is reasonably linear for $[Ru(dpp)_3]Cl_2$, but the corresponding plots for the Pd and Pt porphines exhibit rather sharp curvature in the low oxygen pressure range. The ruthenium dye is interesting because the decay profiles are close to exponential over the entire range of p_{O_2} examined. As a consequence, the fitted distribution parameter γ is small in magnitude and exhibits considerable scatter (Figure 6B) over the range of pressures examined.

(39) Albery, W. J.; Bartlett, P. N.; Wilde, C. P.; Darwent, J. R. *J. Am. Chem. Soc.* **1985**, *107* (7), 1854–1858.

(40) See Figure S3 in the Supporting Information for a comparison of $\tau_m{}^o/\tau_m$ values to $\langle\tau^o\rangle/\langle\tau\rangle$.

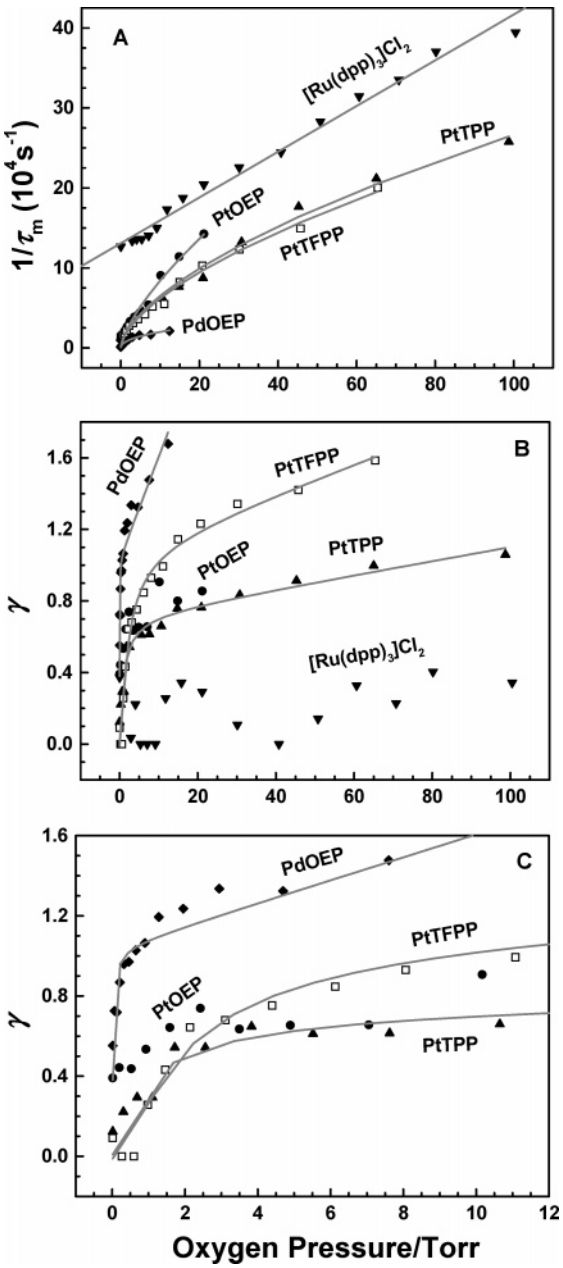

Figure 6. Dependence of the Gaussian model fitting parameters k_m (A) and γ (B) on the oxygen pressure for PtOEP, PtTFPP, PtTPP, PdOEP, and $[Ru(dpp)_3]Cl_2$ adsorbed on the silica TLC plates. In (C), we plot γ values from (B) on an expanded scale to emphasize changes that occur in the low-pressure range.

Variation in Capture Radius for the Different Dyes. In this section, we return to the data in Figure S1 and address the question of why scaling the data by the lifetime of the dye is not sufficient to reduce the quenching data to a common line. Our analysis follows that originally developed in ref 29 to explain the similar phenomena seen in Figure S1B for dyes adsorbed to mesoporous silica. To proceed, we draw an analogy between dyes adsorbed to a surface and dyes dissolved in an elastomeric polymer film. In both systems, the dyes are relatively immobile on the time scale of τ^o and quenching depends on the diffusion of oxygen molecules. The polymer film acts as a viscous liquid, and for diffusion-controlled quenching in three dimensions, the diffusion controlled rate constant k_q can be written as

$$k_q = 4\pi N_A \alpha R_{eff} D_{O_2} \tag{11}$$

Here N_A is Avogadro's number, D_{O_2} is the oxygen diffusion coefficient in the polymer, R_{eff} is the effective interaction distance between the excited dye and quencher at which quenching takes place, and α describes the fraction of encounters that lead to quenching.

Under these circumstances, one can write the Stern−Volmer equation as

$$\frac{1}{\tau^o}\left(\frac{I^o}{I} - 1\right) = 4\pi\alpha R_{eff} N_A P_{O_2} p_{O_2} \tag{12}$$

Here P_{O_2} is the oxygen permeability, equal to the product of D_{O_2} and the Henry's law constant S_{O_2} relating the molar oxygen concentration in the film to the external oxygen pressure ($[O_2] = S_{O_2} p_{O_2}$). In reality, because of multiple collisions, the magnitude of αR_{eff} varies with factors that affect diffusion rates in the system.

Equation 12 can also be used to explain for a series of different dyes why $1/\tau^o$ may not be a sufficient scaling parameter to reduce all the data to a common line, since the dyes may differ in their αR_{eff} values. We used this approach to explain differences in O_2 quenching sensitivity for dyes dissolved in the polar aprotic polymer C_4PATP,[25] where we assumed $\alpha R_{eff} = 1.0$ nm for PtOEP and calculated values of 0.5 for $[Ru(dpp)_3]Cl_2$ and 0.65 nm for PtTFPP.

This idea can be extended to the case of oxygen quenching for dyes adsorbed to the surface of TLC silica by seeking values of αR_{eff} that operate as scaling factors along the y-axis to bring the various quenching curves into proximity. In this instance, the parameter P_{O_2} in eq 12 no longer refers to the traditional "permeability" of a material to oxygen, but rather represents all of the proportionality constants except αR_{eff} connecting the measurable parameters on the left-hand side of the equation to the external oxygen pressure.

In Figure 7 we show that, at low oxygen pressure, the quenching data for all of the dyes will fit a common curve if one plots $[(I^o/I) - 1]/(\alpha R_{eff}\,\tau^o)$ versus p_{O_2}, where the αR_{eff} values are taken relative to 1.0 nm for PtOEP as the best shift factors for curve superposition. The dyes $[Ru(phen)_3]Cl_2$ and $[Ru(phen_3\text{-}phenCH_3)]Cl_2$ show a pronounced downward deviation from the master curve for p_{O_2} values above 20 Torr, and the plots for the other dyes begin to separate above 50 Torr. Nevertheless, this analysis does bring the data for two of the ruthenium dyes and all of the Pd and Pt porphine dyes into better agreement. This behavior is different from what we found for the mesoporous silica, where the data for these six dyes, plotted according to eq 12, fit a common line for the entire range of pressures examined ($p_{O_2} <$ 120 Torr). There, too, deviations were found for $[Ru(phen)_3]Cl_2$ and $[Ru(phen_3phenCH_3)]Cl_2$. Values of αR_{eff} that best fit the data for the dyes on TLC silica and mesoporous silica are presented in Table 1, relative to an assumed value of 1.0 nm for PtOEP. For

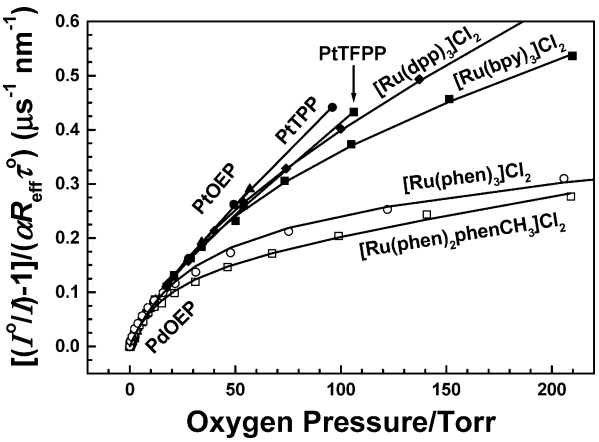

Figure 7. Scaled intensity Stern−Volmer plots $((I^o/I - 1)/(\alpha R_{eff}\tau^o)$ vs $p_{O_2})$ for the dyes adsorbed on the silica TLC plates. Here the scaling parameter employed for each dye is the reciprocal of the product $\alpha R_{eff}\tau^o$. Values of αR_{eff} for each dye were selected relative to an assumed value of 1.0 nm for PtOEP to optimize superposition of the curves.

the TLC silica, these values range from 0.5 for PtTFPP to 2.2 for $[Ru(bpy)_3]Cl_2$ and 2.8 for $[Ru(phen)_3]Cl_2$.

SUMMARY

Literature reports indicate that dyes adsorbed to silica TLC plates can serve as very rapid photoluminescent sensors of changes in air pressure. To give these types of experiments a more quantitative context, we have undertaken a detailed study of phosphorescence quenching by oxygen for eight different dyes adsorbed to the surface of TLC silica and compared the quenching behavior to results reported previously[29] for the same dyes adsorbed to the pore surface of SBA-15 mesoporous silica.

For both systems, the intensity Stern−Volmer plots (I^o/I vs p_{O_2}) were curved, particularly in the range of low oxygen pressures. These data could be fitted well to two phenomenological models proposed by Demas and co-workers,[28] the two-site SV model and the Freundlich isotherm model. The parameters for these fits provide for each dye a calibration curve for experiments in which one wants to convert a measured intensity change to a change in external oxygen pressure. In the absence of oxygen, several of the dyes adsorbed to the TLC silica (PtOEP, PtTFPP, PtTPP, $[Ru(bpy)_3]Cl_2$) exhibited exponential decay profiles, and the PL decay of $[Ru(dpp)_3]Cl_2$ was nearly exponential. Unlike the mesoporous silica substrate, where the lifetime SV plots (τ^o/τ vs p_{O_2}) tracked the intensity SV plots closely, except at the highest oxygen pressures examined, the lifetime SV plots for the dyes adsorbed to the TLC silica were more irregular. For two of the dyes (PtOEP, PtTFPP) the behavior was as described for the mesoporous silica. In contrast, the lifetime plot for PtTPP tracked the intensity plot only to ~10 Torr and then became more sharply curved. Most of the values lie well below the intensity curve. $[Ru(dpp)_3]Cl_2$ is again different. The lifetime plot is nearly linear and lies well below the intensity plot.

This collection of results is difficult to explain in an unambiguous way. In an attempt to rationalize some of the different types of behavior found, we will speculate about some of the features of the dye−substrate interaction. We will assume that the most prominent feature of TLC silica is a distribution of different sites or regions of the surface. One intriguing result was that in the absence of oxygen many of the dyes adsorbed to TLC silica exhibited exponential or nearly exponential PL decay profiles. Even if a given dye has adsorbed a variety of different sites, the dyes bound to these sites are characterized by similar PL decay rates. When oxygen is added to the system, for most of the dyes, the PL decays exhibit a larger distribution of decay rates. The best evidence for this statement is the striking increase in the γ parameter from the Gaussian decay rate distribution analysis as seen in Figure 6B and C. We conclude that the surface variations present in the TLC silica manifest themselves primarily in a distribution of quenching rates by oxygen, rather than as a distribution of intrinsic (unquenched) decay rates for the dyes themselves.

Distributions in quenching kinetics can arise through local variations in oxygen surface concentration, but it is more likely to arise from a distribution of oxygen diffusivities in the system. To understand how this might occur, we refer to insights provided by the experiments of Krasnansky et al.[38] These authors suggest that, from a steady-state point of view, the amount of oxygen adsorbed on the silica surface at ambient temperature in the range where quenching occurs is quite low. In addition, the residence time of oxygen molecules adsorbed to the surface of silica is very short, ranging from a few picoseconds to several hundred picoseconds depending on the temperature. In their view, oxygen molecules from the atmosphere rapidly diffuse onto and depart from the surface, so that the number of times an adsorbed oxygen is replaced at some other arbitrary surface location by an oxygen from the gas phase is great during the lifetime of the dye. They state that this displacement is an essential step in the apparent surface migration of oxygen during the lifetime of the dye's excited state. From this perspective, we can rationalize our finding that dyes adsorbed to TLC silica are 2−3 times more sensitive to oxygen quenching than those located within the pores of SBA-15 mesoporous silica. In SBA-15, the pores are ~1−2 μm in length, as well as narrow (~9 nm) and uniform in diameter. Oxygen diffusion along the pore length within these narrow pores is likely to be much slower because of the confinement effect of the walls than in a more open porous structure. The TLC silica has a more open structure and, as one can see in Figure 2, a broader distribution of pore diameters. We speculate that the enhanced sensitivity to quenching is connected to more rapid diffusion of oxygen in this open pore structure, and the broader distribution of quenching rates is connected to the broader distribution of pore sizes. This feature of the quenching mechanism is also likely to play an important role in applications where the ability of the sensor to respond to a sudden increase or decrease in oxygen partial pressure is critical.

ACKNOWLEDGMENT

The authors thank NSERC Canada and the Royal Canadian Mounted Police for their support of this research.

SUPPORTING INFORMATION AVAILABLE

Lifetime-normalized intensity Stern−Volmer plots for dyes adsorbed to the silica TLC plates and mesoporous SBA-15 silica particles. PL decay profiles for PtOEP, PtTPP, and $[Ru(dpp)_3]Cl_2$ adsorbed to the silica TLC plates as a function of oxygen partial pressure. Comparison of intensity, lifetime, and Gaussian lifetime Stern−Volmer plots. This material is available free of charge via the Internet at http://pubs.acs.org.

Received for review June 30, 2005. Accepted October 19, 2005.

AC0511703